Theory for Nuclear Magnetic Relaxation of Probes in Anisotropic Systems: Application to Cholesterol in Phospholipid Vesicles†

James R. Brainard and Attila Szabo*

ABSTRACT: The nuclear magnetic relaxation of a nucleus in a cylindrical probe embedded in a bilayer vesicle is considered. The probe is assumed to diffuse freely about its unique (C_∞) symmetry axis with an effective correlation time $\tau_\parallel$, and the C_∞ axis moves in a potential which is azimuthally symmetric about a director, with an effective correlation time $\tau_\perp$. The overall isotropic rotational correlation time of the membrane is τ_M. Dipolar relaxation and, in the special case that the relevant tensors are axially symmetric, quadrupolar and chemical shift anisotropy relaxation are treated. An expression for the appropriate correlation function is derived which depends on the above effective correlation times, on the order parameter of the C_∞ axis of the probe, and on the angle (β) which in the case of dipolar relaxation of a protonated ^{13}C nucleus is between the ^{13}C-H vector and the C_∞ axis of the probe. A significant feature of this formulation of the dynamics is that no assumptions need be made concerning the relative order of magnitudes of the effective correlation times and the Larmor frequencies (e.g., such as the extreme narrowing limit). The model not only can be used to describe the dynamics of probes such as cholesterol in membranes but also is applicable to certain anisotropic internal motions in proteins. In addition, by allowing the angle β to fluctuate, a simple model for segmental motion in lipid molecules can be obtained. As an application, ^{13}C nuclear magnetic relaxation experiments on cholesterol in sonicated egg yolk phosphatidylcholine vesicles are interpreted within the framework of the model. The remarkable observation that the protonated C6 carbon has a line width which is much narrower than those of other methine carbons and is in fact comparable to the line width of the nonprotonated C5 carbon is shown to be the consequence of (1) the anisotropic nature of the cholesterol motion in the bilayer and (2) the fact that the angle between the $^{13}C6$-H vector and the long axis of cholesterol is very close to the "magic" value of 54.7°.

Nuclear magnetic resonance (NMR)[1] spectroscopy has been extensively employed during the past decade to study the dynamics and structure of lipid molecules in biological membranes, plasma lipoproteins, and numerous model systems (Bocian & Chan, 1978; Seelig, 1977). Unfortunately, the interpretation of the experimental data from these systems in terms of the physical motions of the lipids is not straightforward because of their anisotropic nature. In addition, the dynamics of many of the constituent lipid molecules are characterized by internal motions, further complicating the interpretation of spectral data. Cholesterol-3α-d_1 has recently been used as a probe in deuterium NMR studies of phospholipid bilayers to circumvent this second problem (Oldfield et al., 1978; Gally et al., 1976). Cholesterol has the advantages that internal motions within the ring system are minimal and that cholesterol and its esters are found naturally in a wide variety of biological systems.

^{13}C NMR spectra of cholesterol and/or cholesterol esters have recently been obtained for a number of biologically relevant systems, including plasma lipoproteins (Hamilton & Cordes, 1978; Avila et al., 1978), arterial plaques (Hamilton et al., 1979), and neat cholesterol esters (Hamilton et al., 1977), complexed with phospholipid in anhydrous triglyceride (H. Oppenheimer and E. H. Cordes, unpublished experiments) and in egg yolk phosphatidylcholine vesicles (Brainard & Cordes, 1981). An interesting feature of ^{13}C NMR spectra of these systems is that under certain conditions the line widths of resonances arising from C3 and/or C9 of the cholesterol ring system are significantly greater than that of C6.

^{13}C NMR spectra of cholesterol in egg yolk phosphatidylcholine vesicles show an additional interesting feature, namely, that the nonprotonated carbon resonance C5 has a line width approximately equal to that for C6 (Brainard & Cordes, 1981). In most ^{13}C NMR spectra, at magnetic field strengths presently available, nonprotonated carbons show signficantly narrower resonances than protonated carbons, a consequence of the greater distance between the nonprotonated carbon and its nearest proton(s) (Norton et al., 1977). Consequently, the observation that a protonated and a nonprotonated carbon in the same rigid ring system show similar line widths is remarkable.

Hamilton et al. (1977) have suggested that the different methine line widths observed in neat cholesterol esters reflect the anisotropic reorientation of the cholesterol ring system, based on the assumption that the ^{13}C relaxation mechanism is dominated by dipolar interactions with directly bonded protons and the fact that C3, C6, and C9 are all methine carbons which are part of the cholesterol ring system. They propose that differences in the rotation rates about the two *short* axes of the cholesterol ring are responsible for the marked divergence of the C3 and C6 line widths which occurs in the isotropic liquid phase as the cholesteric phase transition temperature is approached. However, examination of a space-filling model of cholesterol reveals that the molecular shape is very similar to that of an axially symmetric ellipse. Consequently, a physical basis for different rotational rates about

† From the Department of Medicine, Baylor College of Medicine, Houston, Texas 77030 (J.R.B.), and the Department of Chemistry, Indiana University, Bloomington, Indiana 47405 (A.S.). *Received September 10, 1980; revised manuscript received February 4, 1981.* This work was supported by U.S. Public Health Service Grants GM19631 and HL21483. J.R.B. was supported by National Institutes of Health Postdoctoral Fellowship F32 HL05696. A.S. is an Alfred P. Sloan fellow.

* Address correspondence to this author at the Laboratory of Chemical Physics, National Institute of Arthritis, Metabolism, and Digestive Diseases, National Institutes of Health, Bethesda, MD 20205.

[1] Abbreviations used: NMR, nuclear magnetic resonance; CSA, chemical shift anisotropy; EYPC, egg yolk phosphatidylcholine; DMPC, 1,2-dimyristoyl-1,3-*sn*-phosphatidylcholine; X_{CH}, mole fraction of cholesterol.

0006-2960/81/0420-4618$01.25/0

the short axes is difficult to imagine. In this paper, we examine the relationship between the anisotropic rotation of the cholesterol ring system and the nuclear magnetic relaxation rates of several of its carbon nuclei and suggest a simple and physically reasonable explanation which accounts for the observations that the cholesterol C6 line widths is narrower than that for C3 and/or C9 in a number of systems and that it is approximately equal to that for C5 in EYPC vesicles. Specifically, we propose that these observations are the consequence of the facts (1) that motion of the long axis of the cholesterol molecule is more hindered and/or slower than motion about this axis and (2) that the angle between the ^{13}C6-H internuclear vector and the long axis of the molecule is very close to the "magic" angle, 54.7°.

This proposal is based on the analysis of the following model of the dynamics of an axially symmetric probe embedded in a membrane. We assume that the probe may freely diffuse (with an effective correlation time $\tau_\parallel$) about its unique (C_∞) symmetry axis which in turn may "wobble" (with effective correlation time $\tau_\perp$) in a potential which is azimuthally symmetric about a director attached to the membrane. The membrane may diffuse isotropically with a correlation time τ_M. The angle between the pertinent interaction vector and the C_∞ axis of the probe is β. Although the application of this model in this paper is to cholesterol, the model can be used to describe hindered internal motions of certain amino acid side chains in proteins. Moreover, by allowing the angle β to fluctuate, one obtains a simple model for the dynamics of a phospholipid probe including segmental motion.

The physical content of the above model is essentially the same as that introduced in an important paper by Petersen & Chan (1977). These authors emphasize the significance and interpretation of the order parameter obtained from deuterium NMR. However, their discussion of the dynamics is less complete. They quote expressions relating the deuterium NMR line width which were presumably obtained under a variety of special assumptions about the order of magnitudes of the relaxation times ($\tau_M \gg \tau_\perp \gg \tau_\parallel$) and the Larmor frequencies (i.e., the extreme narrowing limit $\tau_\perp^2\omega^2 < 1$). Our formulation is a more explicit mathematical translation of the physical model and has the advantage that the resulting expressions for the NMR relaxation times are applicable even in the absence of the above-mentioned special conditions. However, we do make the *secular approximation* in calculating the relaxation times. The nonsecular contributions to spin relaxation are negligible when the overall reorientation time is sufficiently fast so that T_1, $T_2 \gg \tau_M$ or else when solid-state effects (e.g., quadrupole splittings) are not observed ($\tau_M < 10^{-5}$ s). While our treatment is valid for bilayer vesicles, it is not applicable to those multilayer liposomes where T_2 and τ_M are the same order of magnitude. Finally, by focusing on a correlation function, our approach treats quadrupolar and chemical shift anisotropy relaxation (when the appropriate tensors are axially symmetric) as well as dipolar relaxation in a unified manner.

The outline of the paper is as follows. First, within the above model of the dynamics, we derive an approximate expression for the correlation function from which the spectral densities and hence the nuclear magnetic relaxation times and, in the case of dipolar relaxation, the nuclear Overhauser effect may be calculated. We show that for special physical situations (such as the C_∞ axis does not "wobble" etc.) our correlation function exactly reduces to those obtained by others (Woessner, 1962a,b; Howarth, 1979; Lipari & Szabo, 1980). Second, for purposes of comparison with previous work on lipids in model membranes (Stockton et al., 1976; Petersen & Chan, 1977), we obtain expressions for the deuterium NMR line width when $\tau_M \gg \tau_\perp \gg \tau_\parallel$, assuming that the extreme narrowing limit is applicable for the "wobbling" motion (i.e., $\tau_\perp^2\omega^2 < 1$). Third, we present illustrative calculations to show how the ^{13}C relaxation times depend on the effective correlation times, the degree of spatial restriction (i.e., the order parameter of the C_∞ axis of the probe), and the angle β, which, in the case of dipolar relaxation, is the angle between the ^{13}C-H vector and the C_∞ axis of the probe. Finally, we show that the results of Brainard & Cordes (1981) can be simply understood within the framework of the model.

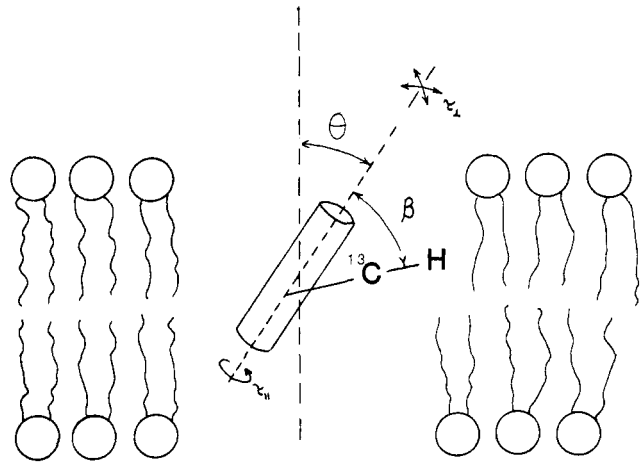

FIGURE 1: Pictorial representation of the physical model for the motion of a ^{13}C–H or C–^{2}H bond in an axially symmetric membrane probe showing the conventions used in describing the motion and geometry of the probe.

Theory

We consider the relaxation of a protonated carbon nucleus rigidly attached to a cylindrical probe embedded within a membrane vesicle. The relaxation mechanism of protonated carbons in magnetic fields less than 150 kG is primarily dipolar (Norton et al., 1977), and the relaxation rates depend on motions which reorient the ^{13}C-H vector with respect to the external magnetic field. The motion of this vector may be described in terms of the probe's geometry and diffusion constants by the coordinate system shown in Figure 1. As shown in this figure, the ^{13}C-H vector is inclined at an angle β with respect to the unique (C_∞) symmetry axis of the probe. The probe may diffuse freely within the membrane about the C_∞ axis with a diffusion constant $D_\parallel$. However, due to the liquid-crystalline nature of the phospholipid bilayer, the motion of the C_∞ axis of the probe is expected to be hindered. We assume that the C_∞ axis diffuses under the influence of a potential [$V(\theta)$] which depends *only* on the angle θ between the C_∞ axis and a director, with a diffusion constant $D_\perp$. Thus, the motion of the probe is axially symmetric about the director which we have chosen to be coincident with the bilayer normal. The simplest choice for this potential is $V(\theta)$ = constant for $0 \le \theta \le \theta_0$, and $V(\theta) = \infty$ otherwise. This is physically equivalent to assuming that the C_∞ axis is restricted to diffuse freely within a cone of semiangle θ_0. Such a model has been used by Kinosita et al. (1977) to describe the dynamics of fluorescent probes in membranes.

Figure 2 shows a carbon *nonrigidly* attached to a spherical macromolecule in such a way that the ^{13}C-H vector may freely rotate about an axis which in turn can "wobble" about a director attached to the macromolecule. If the probe in Figure 1 is embedded in a vesicle which undergoes isotropic rotational motion, the relaxation of the carbons in Figures 1 and 2 is

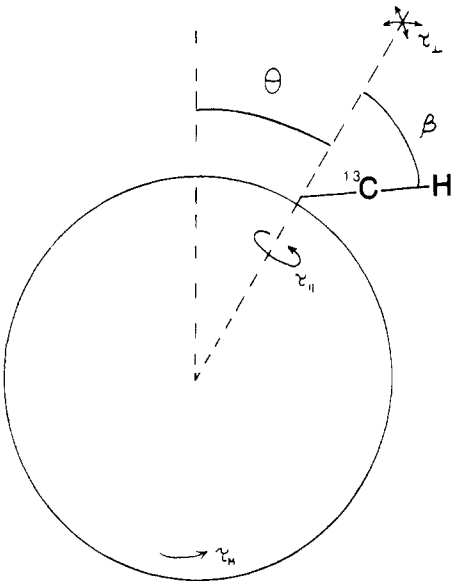

FIGURE 2: Pictorial representation of the physical model as it might apply to describe the dynamics of a side chain within a protein.

identical, provided that the diffusion constant for isotropic rotation of the vesicle is identified with that of the macromolecule. Thus, the mathematical formulation presented below is applicable to both cases. The model in Figure 2 can be used to describe the influence of librational motion of the α carbon on the relaxation of the β carbon of alanines in proteins.

As recently discussed by Lipari & Szabo (1980), the theory of ^{13}C NMR relaxation is quite analogous to the theory of fluorescence depolarization. The problem considered here is essentially the same as the problem of describing the fluorescence emission anisotropy of a cylindrical probe embedded in a membrane for the case in which the emission and absorption dipoles and the C_∞ axis of the probe all point in different directions. The resulting expression for the fluorescence emission anisotropy is quoted in the paper by Lipari & Szabo (1980) and constitutes a generalization of the work of Kinosita et al. (1977).

To obtain the relaxation times within the above model, we derive a useful approximate expression for the correlation function $C(t)$ from which the spectral density, $J(\omega)$, may be calculated via

$$J(\omega) = 2\int_0^\infty \cos(\omega t)C(t)\,dt \tag{1}$$

We use the notation of Wittebort & Szabo (1978) as closely as possible. The expressions for the longitudinal (T_1) and transverse (T_2) relaxation times and the nuclear Overhauser effect can be obtained from their Table I. We begin by introducing the following coordinate systems: (1) the laboratory or L frame; (2) the M frame, which is attached to the membrane (or macromolecule) with the Z_M axis parallel to the director; (3) the D frame, which is attached to the probe with the Z_D axis lying along the C_∞ axis (θ in Figure 1 is the angle between Z_M and Z_D); (4) the F frame, which is attached to the carbon nucleus of interest with the Z_F axis lying along the ^{13}C-H vector (β in Figure 1 is the angle between Z_D and Z_F). We let Ω_{IJ} be the Euler angles which specify the orientation of the J frame with respect to the I frame. The required correlation function is

$$C(t) = \langle D_{qo}^{(2)*}[\Omega_{LF}(0)]D_{qo}^{(2)}[\Omega_{LF}(t)]\rangle \tag{2}$$

where $D_{ab}^{(2)}(\Omega)$ are Wigner rotation matrix elements (Brink & Satchler, 1961). Using the transformation properties of these matrixes, we can write

$$D_{qo}^{(2)}(\Omega_{LF}) = \sum_{a=-2}^{2}\sum_{b=-2}^{2} D_{qa}^{(2)}(\Omega_{LM})D_{ab}^{(2)}(\Omega_{MD})D_{bo}^{(2)}(\Omega_{DF}) \tag{3a}$$

Substituting this into eq 2, assuming that the internal motion of the probe and the overall motion of the vesicle are independent, and using

$$\langle D_{qa}^{(2)*}[\Omega_{LM}(0)]D_{qa'}^{(2)}[\Omega_{LM}(t)]\rangle = \frac{\delta_{aa'}}{5}\exp(-6D_M t) = \frac{\delta_{aa'}}{5}\exp(-t/\tau_M) \tag{3b}$$

where D_M and τ_M ($\tau_M = 1/6D_M$) are the rotational diffusion constant and correlation time, respectively, of the vesicle, one obtains the following equation from eq 2:

$$C(t) = \frac{\exp(-t/\tau_M)}{5}\sum_{abb'}\langle D_{ab}^{(2)*}[\Omega_{MD}(0)]D_{ab'}^{(2)}[\Omega_{MD}(t)]\rangle \times D_{bo}^{(2)*}(\Omega_{DF})D_{b'o}^{(2)}(\Omega_{DF}) \tag{4}$$

Since the motion of the probe is azimuthally symmetric about Z_M (i.e., the potential depends only on θ), the correlation function in eq 4 is nonzero only if $b = b'$. Thus, we may write eq 4 as

$$C(t) = \frac{\exp(-t/\tau_M)}{5}\sum_{b=-2}^{2} C_b(t)[d_{bo}^{(2)}(\beta)]^2 \tag{5}$$

where we have defined

$$C_b(t) = \sum_a \langle D_{ab}^{(2)*}[\Omega_{MD}(0)]D_{ab}^{(2)}[\Omega_{MD}(t)]\rangle \tag{6}$$

and $d_{ab}^{(2)}(\beta)$ are reduced Wigner rotation matrix elements (Brink & Satchler, 1961). The exact evaluation of this correlation function is difficult, even within the framework of a simple model (such as diffusion in a cone). However, we may obtain a useful approximation to $C_b(t)$ which in conjunction with eq 4 can be used to meaningfully interpret experiments.

We begin by showing that the short-time and long-time behavior of $C_b(t)$ can be obtained as equilibrium averages for an arbitrary potential $V(\theta)$. To obtain $C_b(\infty)$, we use the property of correlation functions that

$$\lim_{t\to\infty}\langle A(0)B(t)\rangle = \langle A\rangle\langle B\rangle$$

so that

$$\begin{aligned} C_b(\infty) &= \sum_a \langle D_{ab}^{(2)*}(\Omega_{MD})\rangle\langle D_{ab}^{(2)}(\Omega_{MD})\rangle \\ &= |\langle D_{oo}^{(2)}(\Omega_{MD})\rangle|^2\delta_{bo} \\ &= \langle d_{oo}^{(2)}(\theta)\rangle^2\delta_{bo} = \langle P_2(\cos\theta)\rangle^2\delta_{bo} \end{aligned} \tag{7}$$

where we have used the fact that the probe moves in a potential which depends only on θ and $P_2(x)$ is the second Legendre polynomial, i.e.

$$d_{oo}^{(2)}(x) = P_2(x) = \frac{3x^2 - 1}{2} \tag{8}$$

The equilibrium average in eq 7 is defined as

$$\langle P_2(\cos\theta)\rangle = \frac{\int_0^\pi p_{eq}(\theta)P_2(\cos\theta)\sin\theta\,d\theta}{\int_0^\pi p_{eq}(\theta)\sin\theta\,d\theta} \tag{9}$$

where $p_{eq}(\theta)$ is the equilibrium orientational distribution function of the probe, i.e.

$$p_{eq}(\theta) \propto \exp[-V(\theta)/k_BT] \quad (10)$$

where k_B is Boltzmann's constant.

We note that $\langle P_2(\cos\theta)\rangle$ is commonly called the order *parameter*, S, of the probe, i.e.

$$S = \langle P_2(\cos\theta)\rangle \quad (11)$$

The concept of an order parameter plays a central role in the interpretation of electron spin resonance and deuterium NMR (^{2}H NMR) studies of membranes (Petersen & Chan, 1977; Bocian & Chan, 1978). To avoid possible confusion, we note that the relation between our notation and that of Petersen & Chan (1977) is as follows: our β corresponds to their γ while our θ corresponds to their α (thus, their S_α is our S). Since knowledge of S alone does not uniquely determine the $p_{eq}(\theta)$, a common approach to extracting physical information from S is to assume a form for $p_{eq}(\theta)$ containing a single adjustable parameter, evaluate $\langle P_2(\cos\theta)\rangle$, and then determine this parameter by using eq 11. For example, for the diffusion in a cone model, $p_{eq}(\theta)$ = constant for $0 \le \theta \le \theta_0$ and zero otherwise. For this model

$$S_{cone} = (1/2)\cos\theta_0(1 + \cos\theta_0) \quad (12)$$

where θ_0 is the cone semiangle. More realistic, but still ad hoc, choices for $p_{eq}(\theta)$ such as $p_{eq}(\theta) \propto \exp[-{}^1/_2(\theta/\theta_0)^2]$ can and have been used (Petersen & Chan, 1977) in this context.

Having expressed the long-time limit of $C_b(t)$ in terms of the order parameter of the probe, we now consider its short-time behavior. Recall that the probe is assumed to diffuse freely about its C_∞ axis with a diffusion constant $D_\parallel$, and the C_∞ axis "wobbles" with diffusion constant $D_\perp$ in a potential $V(\theta)$ (i.e., the dynamics are described by the Smoluchowski equation). We can then show that the short-time behavior of $C_b(t)$, which is exact to linear order in time, is

$$C_b(t) = 1 - t(6D_\perp - b^2D_\perp + b^2D_\parallel) + \ldots \quad (13)$$

independent of the form of $V(\theta)$. The derivation is quite involved and is omitted.

Using the above expressions (eq 7 and 13) for the limiting behavior for $C_b(t)$, we now construct an interpolation formula (essentially a time-dependent Padé approximant) valid for all times which is exact at $t = \infty$ and to linear order in time. As can be readily verified, the appropriate expression is

$$C_b(t) = \exp(-b^2D_\parallel t)\{S^2 + (1 - S^2)\exp[-(6 - b^2)D_\perp t/(1 - S^2)]\} \quad (14)$$

Substituting this into eq 5, we arrive at our major theoretical result

$$C(t) = \frac{1}{5}\exp(-t/\tau_M)\sum_{b=-2}^{2}\exp(-b^2t/6\tau_\parallel) \times \{S^2 + (1 - S^2)\exp[-(t - b^2t/6)/\tau_\perp]\}[d_{bo}^{(2)}(\beta)]^2 \quad (15)$$

where $\tau_\parallel$ ($=1/6D_\parallel$) is the correlation time for diffusion about the C_∞ axis and the effective correlation time ($\tau_\perp$) for the "wobbling" of the C_∞ axis is

$$\tau_\perp = (1 - S^2)/6D_\perp \quad (16)$$

The reduced Wigner rotation matrix element $d_{oo}^{(2)}(\beta)$ is given in eq 8 while (Brink & Satchler, 1961)

$$d_{\pm10}^{(2)}(\beta) = \mp(3/2)^{1/2}\sin\beta\cos\beta \quad (17a)$$

$$d_{\pm20}^{(2)}(\beta) = (3/8)^{1/2}\sin^2\beta \quad (17b)$$

As a result of the symmetry of these matrixes, the terms with $b = \pm1$ and $b = \pm2$ are identical in eq 15.

An important feature of eq 15 is that it explicitly contains the order parameter. Although eq 15 is an approximation, it contains the correct physics of the problem as indicated by the following properties: (1) When the C_∞ axis does not move, our model is physically identical with the situation in which a ^{13}C-H vector with one internal rotation is rigidly attached to an isotropically rotating sphere (Woessner, 1962a). Indeed, when $S = 1$ *or* $\tau_\perp = \infty$, eq 15 reduces to

$$C(t) = \frac{1}{5}\exp(-t/\tau_M)\sum_{b=-2}^{2}\exp(-b^2t/6\tau_\parallel)[d_{bo}^{(2)}(\beta)]^2 \quad (18)$$

which is equivalent to the result of Woessner (1962a). (2) When the motion of the C_∞ axis is entirely unrestricted ($S = 0$) and the membrane or macromolecule does not rotate ($\tau_M = \infty$), the motion of the probe is physically identical with that of a freely diffusing axially symmetric ellipse. Indeed, when $S = 0$ and $\tau_M = \infty$, eq 15 reduces to

$$C(t) = \frac{1}{5}\sum_{b=-2}^{2}\exp[-t(b^2/6\tau_\parallel - b^2/6\tau_\perp + \tau_\perp^{-1})][d_{bo}^{(2)}(\beta)]^2 \quad (19)$$

which is equivalent to the expression derived by Woessner (1962b) for an axially symmetric ellipse. (3) When $\beta = 0$ (i.e., the ^{13}C-H vector is coaxial with the C_∞ axis), rotational diffusion about the C_∞ axis has no effect on the relaxation. Indeed, when $\beta = 0$, eq 15 reduces to

$$C(t) = \frac{1}{5}\exp(-t/\tau_M)[S^2 + (1 - S^2)\exp(-t/\tau_\perp)] \quad (20)$$

so that $\tau_\parallel$ drops out. If S is replaced by S_{cone} (see eq 12), eq 20 has the same form as the expressions obtained by Howarth (1979) ($\tau_\perp \to \tau_G$) and by Lipari & Szabo (1980) ($\tau_\perp \to \tau_{eff}$), using different approaches, for the "wobbling" of α carbon within the framework of the diffusion in a cone model. In contrast to Howarth (1979), Lipari & Szabo (1980) emphasize that eq 20 is appropriate only when the ^{13}C-H vector is coaxial with the wobbling axis. Lipari & Szabo (1980) derive a relationship between $\tau_\perp$ and $D_\perp$ (D_w in their notation) which is different from eq 16. The reason for this is that eq 16 is based on the requirement that the correlation function is exact to linear order in time, whereas Lipari & Szabo (1980) chose their effective correlation time so that the area under the correlation function is exact. For the diffusion in a cone model, the difference between the two expressions is not great. This difference is an increasing function of the cone angle; for $\theta_0 = 60°$, the diffusion coefficient, $D_\perp$, calculated from an effective correlation time by using eq 16 differs from their result by a factor of 1.5. Because of this ambiguity, when applying eq 15 to the analysis of experimental data, we feel that it is appropriate to regard $\tau_\perp$ and $\tau_\parallel$ as *effective* correlation times and not to translate these into diffusion constants by using eq 16.

Recently, Howarth (1979) considered the situation shown in Figure 2 within the framework of the cone model. His expression for $C(t)$ in our notation is

$$C(t) = \frac{1}{5}\exp(-t/\tau_M)[S_{cone}^2 + (1 - S_{cone}^2)\exp(-t/\tau_\perp)]\{\sum_{b=-2}^{2}\exp(-b^2t/6\tau_\parallel)[d_{bo}^{(2)}(\beta)]^2\} \quad (21)$$

which differs from eq 15 when it is specialized to the diffusion in a cone model (i.e., $S \to S_{cone}$). In obtaining eq 21, Howarth argued that the librational motion of the C_∞ axis and the rotational motion about this axis should be independent, and hence he simply multiplied eq 20 by eq 18 (the factor resulting from the overall reorientation of the macromolecule is, of

course, included only once). At first sight, the assumption of independence seems reasonable. However, the situation is more subtle. For example, the correlation function for a freely diffusing axially symmetric ellipse (see eq 19) *cannot* be written as a single product of two terms, one containing only $\tau_\parallel$ and the other only $\tau_\perp$. Indeed, an important objection to Howarth's result (eq 21) is that it does not reduce to eq 19 when the wobbling motion is unrestricted (i.e., $S_{cone} = 0$). In addition, when $\tau_\parallel$ is set equal to infinity in eq 21, the dependence of β disappears, and eq 21 reduces to eq 20. However, even when there is no motion about the C_∞ axis, the motion of the ^{13}C-H vector in Figure 2 is different for different values of β. An analogous situation arises in the Wallach (1967) model for multiple internal rotations. If the correlation time for the ith ($i \neq 1$) internal rotation is set equal to infinity in his expression for the correlation function, the angle between the ith and ith + 1 rotational axis does not drop out. In spite of these unsatisfactory features of Howarth's results, eq 15 and 21 can lead to similar numerical results in a number of cases of interest.

Although the correlation function in eq 15 can be used to calculate the NMR relaxation times without any assumptions about the relative order of magnitudes of τ_M, $\tau_\parallel$, $\tau_\perp$, and the Larmor frequencies, it is of interest to examine some special cases. In the limit that the rotational motion about the C_∞ axis is very fast (i.e., $\tau_\parallel \to 0$), eq 15 becomes

$$C(t) = \frac{1}{5}\exp(-t/\tau_M)[P_2(\cos\beta)]^2[S^2 + (1 - S^2)\exp(-t/\tau_\perp)] \quad (22)$$

Moreover, when $\tau_M \gg \tau_\perp$, eq 22 further simplifies to

$$C(t) = \frac{1}{5}\exp(-t/\tau_M)[P_2(\cos\beta)]^2S^2 + \frac{1}{5}\exp(-t/\tau_\perp)[P_2(\cos\beta)]^2(1 - S^2) = C_M(t) + C_\perp(t) \quad (23)$$

For the case where τ_M is sufficiently long so that only $J_M(0)$ contributes to the line width and where $\tau_\perp$ is sufficiently short so that the extreme narrowing limit applies to the wobbling motion [i.e., $J_\perp(0) = J_\perp(\omega_C) = ...$, etc.), we have [see Table I of Wittebort & Szabo (1978)]

$$\Delta\nu(^{13}\text{C-H}) = (\pi T_2)^{-1} = K_{^{13}\text{C-H}}[J_M(0) + 5J_\perp(0)] = 2K_{^{13}\text{C-H}}\left[\int_0^\infty C_M(t)\,dt + 5\int_0^\infty C_\perp(t)\,dt\right] \quad (24)$$

where

$$K_{^{13}\text{C-H}} = \frac{1}{2\pi}\hbar^2\gamma_C^2\gamma_H^2 r_{CH}^{-6} \quad (25)$$

Using eq 23 in eq 24 and evaluating the integrals, we have

$$\Delta\nu(^{13}\text{C-H}) = \frac{2}{5}K_{^{13}\text{C-H}}[P_2(\cos\beta)]^2[S^2\tau_M + 5(1 - S^2)\tau_\perp] \quad (26a)$$

This is an important result. It shows how the line width depends on the angle between the ^{13}C-H vector and the C_∞ axis of the probe (i.e., β). When β is close to the magic angle (54.7°), the line width is very narrow (see below). It must be kept in mind that $\tau_\perp$ in eq 26a is an *effective* correlation time [i.e., it depends not only on the diffusion constant for the wobbling of the C_∞ axis but also on certain averages involving the potential [$V(\theta)$] in which the C_∞ axis moves]. We have not been able to find a general, analytical relationship between $\tau_\perp$ and the diffusion constant. However, when the dynamics of the probe are described as diffusion (with diffusion constant D_w) in a cone of semiangle θ_0, and $\tau_M \gg \tau_\perp$, $J_\perp(0)$ has been *exactly* evaluated by Lipari & Szabo (1980). Thus, within this model, the exact version of eq 26 is

$$\Delta\nu(^{13}\text{C-H}) = \frac{2}{5}K_{^{13}\text{C-H}}[P_2(\cos\beta)]^2(S_{cone}^2\tau_M + 5F\tau_w) \quad (27a)$$

where

$$F = -3x_0^2(1 + x_0)^2[\log[(1 + x_0)/2] + (1 - x_0)/2]/(1 - x_0) + (1 - x_0)(6 + 8x_0 - x_0^2 - 12x_0^3 - 7x_0^4)/4 \quad (28)$$

where $x_0 = \cos\theta_0$ and $\tau_w = 1/6D_w$.

Up to this point, we have focused on the dipolar relaxation of ^{13}C nuclei. However, our development is also applicable to quadrupolar and chemical shift anisotropy (CSA) relaxation in the special case that relevant tensors are axially symmetric. In the case of CSA relaxation, β is the angle between the unique axis of the chemical shift anisotropy tensor and the C_∞ axis of the probe. In deuterium NMR, if the quadrupolar interaction tensor is symmetric about the C–^{2}H bond, β is the angle between the C–^{2}H bond and the C_∞ axis of the probe. For both these relaxation mechanisms, the expressions relating T_1 and T_2 to the spectral densities obtained from eq 15 via eq 1 can also be found in Table I of Wittebort & Szabo (1978).

For purposes of comparison to previous work, we present expressions for the ^{2}H NMR line width which are analogous to eq 26a and 27a. The results are

$$\Delta\nu(\text{C-}^2\text{H}) = \frac{9}{80\pi}\left(\frac{eqQ}{\hbar}\right)^2[P_2(\cos\beta)]^2\left[S^2\tau_M + \frac{10}{3}(1 - S^2)\tau_\perp\right] \quad (26b)$$

and

$$\Delta\nu(\text{C-}^2\text{H}) = \frac{9}{80\pi}\left(\frac{eqQ}{\hbar}\right)^2[P_2(\cos\beta)]^2\left(S^2\tau_M + \frac{10}{3}F\tau_w\right) \quad (27b)$$

The first term (involving τ_M) in the above equations is the same as the first term of eq 25 of Petersen & Chan (1977) which in turn is equivalent to the second term of eq 14 of Stockton et al. (1976). Actually, both Stockton et al. (1976) and Petersen & Chan (1977) consider the possibility that the probe undergoes lateral diffusion within the membrane. Our expressions can be generalized to include this effect simply by replacing τ_M^{-1} with $\tau_M^{-1} + \tau_d^{-1}$ where τ_d is the correlation time for translational diffusion. The second term in eq 26b (involving $\tau_\perp$) does not appear to be equivalent to the corresponding term quoted by Petersen & Chan (1977) without a derivation. Our second term is simply $(\pi T_1)^{-1}$ calculated for the model shown in Figure 1 (with $\tau_\parallel \to 0$), assuming that the extreme narrowing limit is applicable to the wobbling motion, i.e.

$$\frac{1}{\pi T_1} = \frac{3}{8\pi}\left(\frac{eqQ}{\hbar}\right)^2[P_2(\cos\beta)]^2(1 - S^2)\tau_\perp \quad (29a)$$

This is to be compared with the recent result of Brown et al. (1979)

$$\frac{1}{\pi T_1} = \frac{3}{8\pi}\left(\frac{eqQ}{\hbar}\right)^2(1 - S_{CD}^2)\tau_c \quad (30)$$

where S_{CD} is the order parameter of a C–^{2}H bond in a fatty acyl chain in a bilayer and τ_c is an effective correlation time describing the motion of this bond. For the model shown in Figure 1

$$S_{CD} = SP_2(\cos\beta) \quad (31)$$

Thus, eq 30 and 29a are not quite identical. The reason for this is that $\tau_\perp$ and τ_c are different *effective* correlation times. Within the diffusion in the cone model, the exact expression corresponding to eq 29a is

$$\frac{1}{\pi T_1} = \frac{3}{8\pi}\left(\frac{eqQ}{\hbar}\right)^2 [P_2(\cos\beta)]^2 F \tau_w \qquad (29b)$$

where now τ_w is no longer an effective correlation time (i.e., it is related to the wobbling diffusion constant D_w by $\tau_w = 1/6D_w$) but F is a rather complicated expression given in eq 28 which is clearly not equal to $1 - S_{cone}^2$. These considerations show that the interpretation of effective correlation times is not straightforward. The precise relationship between the effective correlation time and the true correlation time (which is simply related to a microscopic diffusion coefficient) depends on the form of the potential, $V(\theta)$, in which the probe moves. Moreover, even for a simple model such as diffusion in a cone, this dependence is rather complicated (see eq 28 for F).

It should be reemphasized that eq 26a,b and 29a,b were obtained from the correlation function in eq 15 in the special case that $\tau_M \gg \tau_\perp \gg \tau_\parallel$ and $\tau_\perp^2\omega^2 < 1$. However, eq 15 is applicable to cases where these conditions are not met as long as τ_M is sufficiently fast so that the nonsecular contributions are negligible. Thus, the present development can be regarded as a dynamical formulation of the model considered by Petersen & Chan (1977).

Finally, we mention a generalization of our treatment. Up to this point, we have assumed that the angle β between the ^{13}C-H or C-^{2}H vector and the C_∞ axis is fixed. A simple model for segmental motion of fatty acyl chains in bilayers can be obtained by allowing β to fluctuate. The appropriate correlation function for this model is given by eq 15 when $[d_{bo}^{(2)}(\beta)]^2$ is replaced by $\langle D_{bo}^{(2)*}[\Omega_{DF}(0)] D_{bo}^{(2)}[\Omega_{DF}(t)]\rangle$. This correlation function can be either approximated by using the order parameter–effective correlation time approach used in this paper or evaluated by using some simple model (e.g., the interaction vector jumps between two orientations or diffuses in a cone). For example, if the interaction vector jumps, with rate constant k, between two equivalent sites with orientations β_1, ϕ_1 and β_2, ϕ_2 with respect to the C_∞ axis, one has

$$\langle D_{bo}^{(2)*}[\Omega_{DF}(0)] D_{bo}^{(2)}[\Omega_{DF}(t)]\rangle = C_b(\infty) + [C_b(0) - C_b(\infty)]e^{-2kt}$$

where

$$C_b(\infty) = \frac{1}{4}\{[d_{bo}^{(2)}(\beta_1)]^2 + [d_{bo}^{(2)}(\beta_2)]^2 + 2 d_{bo}^{(2)}(\beta_1) d_{bo}^{(2)}(\beta_2) \cos b(\phi_1 - \phi_2)\}$$

and

$$C_b(0) = \frac{1}{2}\{[d_{bo}^{(2)}(\beta_1)]^2 + [d_{bo}^{(2)}(\beta_2)]^2\}$$

Alternatively, if the interaction vector diffuses (with diffusion constant D_w) in a cone of semiangle θ_0 about a fixed director, one has

$$\langle D_{bo}^{(2)*}[\Omega_{DF}(0)] D_{bo}^{(2)}[\Omega_{DF}(t)]\rangle = \sum_{c=-2}^{2} [d_{bo}^{(2)}(\beta_0)]^2 \{G_c(\infty) + [G_c(0) - G_c(\infty)]e^{-t/\tau_{eff}^{(c)}}\}$$

where β_0 is the angle between the fixed director and the C_∞ axis of the probe. Explicit expressions for $G_c(\infty)$, $G_c(0)$, and $\tau_{eff}^{(c)}$ in terms of θ_0 and D_w are given by Lipari & Szabo (1981). It is of interest to note that in the case where the interaction vector fluctuates very rapidly compared to $\tau_\perp$, eq 23 (and hence eq 26a,b, 27a,b, and 29a,b which were derived from it) can be rigorously generalized simply by replacing $[P_2(\cos\beta)]^2$ with the square of the corresponding order parameter [i.e., $\langle P_2(\cos\beta)\rangle^2$].

Even without the above generalization, our model is more sophisticated than that of Gent & Prestegard (1977). These authors describe the anisotropic motion of the ^{13}C-H or C-^{2}H vector by a single correlation time (τ_D in their notation) instead of using two correlation times (i.e., $\tau_\parallel$ and $\tau_\perp$). They assume that the tip of the interaction vector moves on an annulus of semiangle Δ (i.e., the part of the surface of the sphere for which $\pi/2 - \Delta \le \theta \le \pi/2 + \Delta$, $0 \le \varphi \le 2\pi$). The correlation function of their model can be obtained from eq 20 by (1) identifying our τ_M with their τ_c, (2) *formally* setting our $\tau_\perp$ equal to their τ_D, and (3) evaluating the order parameter S over the annular region, i.e., setting S equal to

$$S_{annulus} = \frac{\int_{(\pi/2)-\Delta}^{(\pi/2)+\Delta} \sin\theta\, d\theta\, P_2(\cos\theta)}{\int_{(\pi/2)-\Delta}^{(\pi/2)+\Delta} \sin\theta\, d\theta} = \frac{1}{2}\cos^2\Delta \qquad (32)$$

The relationship between the effective correlation time τ_D and the microscopic diffusion constant for the Gent–Prestegard diffusion-in-an-annulus model could be found the same way Lipari & Szabo (1980) derived such a relation for the diffusion-in-a-cone model.

Illustrative Calculations

In this section, we examine the relationship between the parameters describing the motion and geometry of a cylindrically symmetric probe in a membrane and the experimentally observable NMR relaxation rates. Subsequently, we will apply the model and formulation derived in the preceding section to interpret the ^{13}C relaxation rates measured for cholesterol in phospholipid vesicles (Brainard & Cordes, 1981) in terms of the dynamics and geometry of the cholesterol molecule. We begin by numerically illustrating the effects that varying the motion of the cholesterol molecule and the geometry of the ^{13}C-H internuclear vector have upon the predicted relaxation rates. We consider the influence of the following: (1) the rate of motion (i.e., the values for the correlation times); (2) the degree of anisotropy of the motion (i.e., the order parameter characterizing the angular restriction of the C_∞ axis); (3) the orientation of the interaction vector with respect to the major axis of rapid anisotropic motion (i.e., the angle β between the ^{13}C-H internuclear vector and the C_∞ axis). For example, Figure 3 illustrates the effects of varying $\tau_\parallel$, $\tau_\perp$ ($\tau_\parallel = \tau_\perp$), and τ_M upon the natural line width and spin–lattice relaxation time for a methine carbon of a membrane probe. We have assumed, for illustrative purposes, that $\tau_\perp = \tau_\parallel$. The line width is fairly insensitive to the ratio $\tau_\parallel/\tau_\perp$ over a 100-fold range (see Figure 4). The orientation of the ^{13}C-H internuclear vector relative to the C_∞ axis is 60°; other orientations will be discussed later. Each line in this figure corresponds to a different value for τ_M. This figure shows that for a given rate of vesicle rotation, decreased rates of probe motion within the bilayer are associated with larger natural line widths and the usual biphasic dependence of the spin–lattice relaxation time. Decreased rates of vesicle rotation are associated with increases in natural line widths, but spin–lattice relaxation times are relatively independent of the rate for vesicle rotation. Also noteworthy is the observation that for inclinations of the internuclear vector not nearly identical with the magic angle (such as in this case, 60°), the line width is insensitive to $\tau_\parallel$ and $\tau_\perp$ when these correlation times become less than the inverse Larmor frequency. In addition, the line widths are

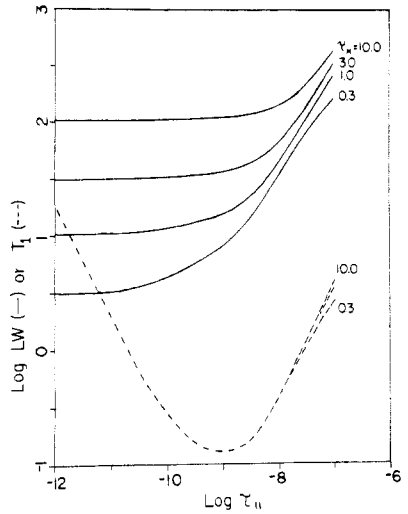

FIGURE 3: Log–log plots of natural line widths $(\pi T_2)^{-1}$ and spin–lattice relaxation times for a methine carbon rigidly fixed to an axially symmetric membrane probe which is embedded within a vesicle membrane vs. the effective correlation time ($\tau_{\parallel}$) for rotation of the probe about its C_∞ axis ($\tau_{\parallel} = \tau_{\perp}$). Families of lines correspond to variations in the rotational correlation time for vesicle tumbling (τ_M). The τ_M values are given in microseconds next to the appropriate line-width plot; the T_1 plots are coincident. The magnetic field strength is 6.3T, relaxation occurs through dipolar interactions with a single proton nucleus 1.09 Å distant, the ^{13}C-H internuclear vector is oriented 60° from the C_∞ axis of the probe, the order parameter for the motion of the C_∞ axis about the membrane director is 0.7, and we have allowed $\tau_{\parallel}$ to vary with $\tau_{\perp}$ ($\tau_{\parallel} = \tau_{\perp}$). The T_1 values and line widths in this and subsequent figures were not calculated by using eq 26a, 27a, and 29a but rather by using the expressions in Table I of Wittebort & Szabo (1978).

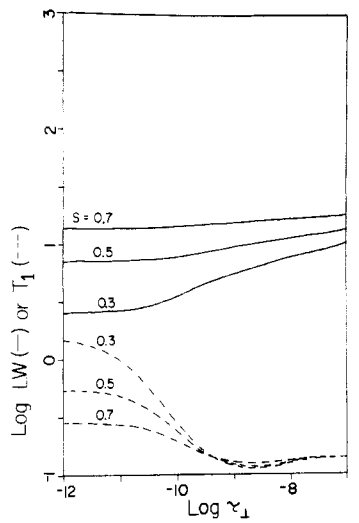

FIGURE 4: Log–log plots of natural line widths and spin–lattice relaxation times vs. the effective correlation time for motion of the C_∞ axis of the membrane probe ($\tau_{\perp}$). Families of lines correspond to different values of the order parameter, as indicated next to each line. The effective correlation time for rotation of the probe about its C_∞ axis ($\tau_{\parallel}$) was held constant at 10^{-9} s. $\tau_M = 10^{-6}$ s; other parameters are as described in Figure 3.

not particularly sensitive to $\tau_{\perp}$, over even a wider range. This is illustrated in Figure 4 where line widths and spin–lattice relaxation times are plotted as a function of $\tau_{\perp}$, holding $\tau_{\parallel}$ equal to 10^{-9} s, for various values of the order parameter. It is clear that when the motion of the C_∞ axis is moderately restricted, $S \geq 0.4$, the line width is only slightly sensitive to changes in $\tau_{\perp}$. In addition, for $\tau_{\perp} > 10^{-10}$ s, T_1 is fairly insensitive both to the order parameter and to $\tau_{\perp}$. Seiter & Chan (1973) have previously noted the differing sensitivities of spin–lattice relaxation times and line widths to the faster

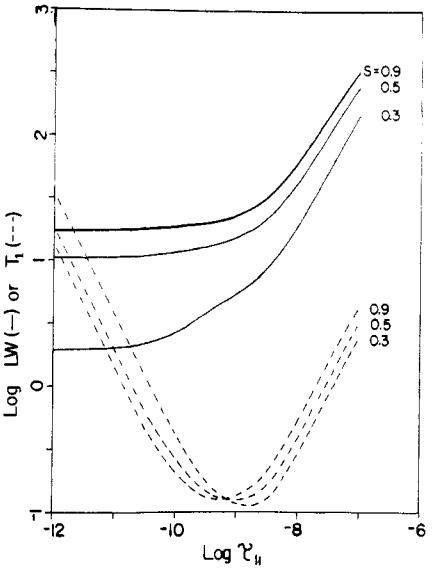

FIGURE 5: Log–log plots of natural line widths and spin–lattice relaxation times vs. the effective correlation time for rotation of the probe about its C_∞ axis ($\tau_{\parallel} = \tau_{\perp}$). Families of lines correspond to different values for the order parameter, S, describing the distribution of the C_∞ axis with respect to the membrane director. The magnitude of S is given next to the appropriate line. $\tau_M = 10^{-6}$ s; other parameters are as described in Figure 3.

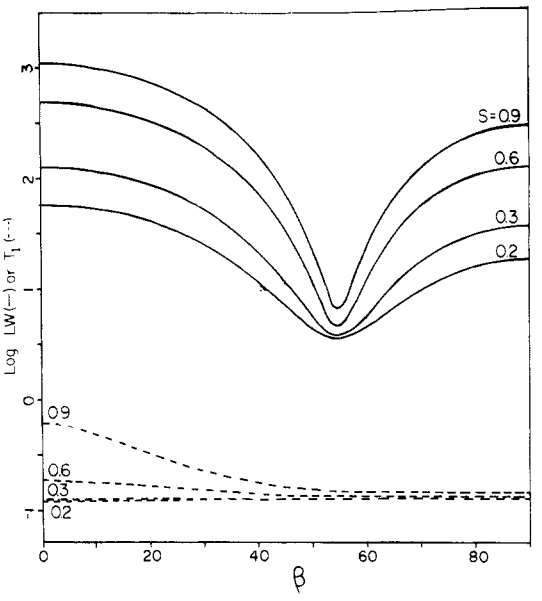

FIGURE 6: Semilog plots of natural line widths and spin–lattice relaxation times vs. the angle β between the ^{13}C-H internuclear vector and the C_∞ axis of the probe. Families of lines correspond to different values of the order parameter S which are given next to the appropriate line. $\tau_M = 10^{-6}$ s and $\tau_{\parallel} = \tau_{\perp} = 10^{-9}$ s; other parameters are as described in Figure 3.

and slower components of motion in anisotropic systems.

The effect of varying the angular restrictions in the motions of the cholesterol long axis is illustrated by the families of lines shown in Figure 5. Each line corresponds to a different value for the order parameter. The degree of anisotropy in the motion of the C_∞ axis affects both the spin–lattice relaxation time and the line width of a methine carbon. Increases in the order parameter characterizing the hindered motion of the C_∞ axis are associated with increased line widths and shift the entire spin–lattice relaxation time curve toward shorter correlation times.

The importance of geometrical considerations in determining the relaxation rates is demonstrated in Figure 6. This figure

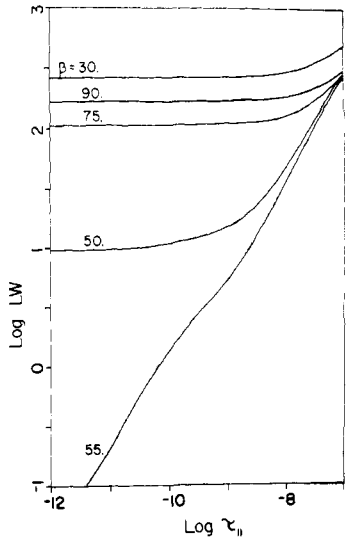

FIGURE 7: Log–log plots of natural line widths and spin–lattice relaxation times vs. the effective correlation time for rotation of the probe about its C_∞ axis ($\tau_\parallel = \tau_\perp$). Families of lines correspond to different orientations of the ^{13}C-H internuclear vector with respect to the C_∞ axis of the probe. $\tau_M = 10^{-6}$ s; other parameters are as described in Figure 3.

shows the dependence of the line width and spin–lattice relaxation times of a methine carbon upon the angle β which describes the orientation of the ^{13}C-H internuclear vector with respect to the C_∞ axis of the probe. Each line in the figure corresponds to a different value for the order parameter, ranging from $S = 0.9$ to $S = 0.2$. It is clear that the orientation of the interaction vector is critically important in determining the relaxation rates, even in systems where the order parameter is fairly small.

We have already suggested that changes in the dynamics of a membrane probe may not necessarily be reflected in the NMR relaxation rates. This observation is further examined in Figure 7. These calculations show that the sensitivity of the line width to fast rotation about the C_∞ axis is determined by the orientation of the interaction vector with respect to that axis. For vectors oriented close to the magic angle, the line width remains sensitive to rotations about that axis which are faster than the Larmor frequency. For vectors inclined at angles other than 55°, the sensitivity of the line width to changes in $\tau_\parallel$ for $\tau_\parallel^2\omega^2 < 1$ decreases (i.e., the slope of the curve approaches zero). This figure emphasizes the importance of geometrical considerations in determining the suitability of a particular probe or a particular nuclear resonance as a sensitive indicator of dynamic changes in anisotropic systems.

Application to Cholesterol Dynamics

We now apply these results to help understand how the ^{13}C relaxation rates for cholesterol in sonicated egg yolk phosphatidylcholine vesicles relate to the dynamics of cholesterol in this system. A noteworthy feature of the spectra of cholesterol in sonicated vesicles is the absence of resonances from cholesterol C9 and C3 in spectra obtained under conditions where the resonance from C6 is easily detected. Brainard & Cordes (1981) have suggested that these resonances are not detected because of the short spin–spin relaxation time of these nuclei and the resulting large natural line width relative to C6. Examination of a CPK molecular model for cholesterol reveals that the ^{13}C-H internuclear vectors for C9 and C3 are oriented at angles close to 90° from the long axis of the cholesterol molecule. The commonly used numbering scheme for cholesterol is

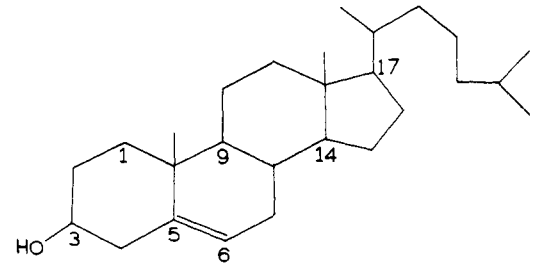

C6 is unique among the protonated carbons of the cholesterol ring system in that its ^{13}C-H internuclear vector is oriented approximately 55° from the cholesterol long molecular axis. Rotation about that axis will result in much smaller line widths for C6 than for the other methine carbon resonances. We propose that the difference between the line widths of cholesterol C6 and C3, C9 is simply a consequence of (1) the orientation of their respective ^{13}C-H vectors with respect to the cholesterol long axis and (2) the anisotropic nature of the cholesterol motion in the bilayer.

The similar line width of the protonated C6 resonance and the nonprotonated C5 in spectra of cholesterol–EYPC vesicles may also be understood within the framework of this model. Although chemical shift anisotropy is usually not an important relaxation mechanism for protonated carbons at the magnetic field strengths presently available (Norton et al., 1977), the field dependence of the line width for cholesterol C6 in sonicated vesicles suggests that CSA might be a contributing relaxation mechanism for this nucleus (Brainard & Cordes, 1981). If the interaction vector for chemical shift anisotropy relaxation was inclined at an angle other than 55° from the cholesterol long axis, CSA could conceivably dominate the relaxation mechanism for cholesterol C6. Unfortunately, the chemical shift tensors for cholesterol C6 are not known. In order to demonstrate that under certain conditions chemical shift anisotropy may contribute significantly to the relaxation mechanism of a protonated carbon, we have assumed that the CSA relaxation rates for cholesterol C6 and C5 may be estimated by using an axially symmetric chemical shift tensor whose magnitude and orientation were estimated from the tensors for C2 of propylene (Appleman & Dailey, 1974). For C2 of propylene and other olefinic nuclei, the largest element of the CSA tensor is approximately perpendicular to the carbon–carbon double bond. Assuming ideal sp^2 geometry about cholesterol C6, one finds that the angle between the symmetry axis of the CSA tensor and the C_∞ axis is 30° larger than the angle (β) between the ^{13}C6-H vector and the C_∞ axis. Calculated spin–spin relaxation rates for dipolar and CSA relaxation as a function of β are shown in Figure 8 for $S = 0.7$. It is clear from this figure that as β approaches 54.7°, the dominant contribution to the spin–spin relaxation time is from chemical shift anisotropy. The conclusion that for orientations of the C6-H internuclear vector close to 54.7° from the C_∞ axis, CSA may contribute significantly to the spin–spin relaxation rate of cholesterol C6 is not critically dependent on the precise orientation and magnitude of the chemical shift tensor or on the values for the correlation times and order parameter.

Figure 9 compares the calculated natural line widths and spin–lattice relaxation times for cholesterol C5 and C6 as a function of β. These calculations were based upon the assumptions that relaxation of C5 occurs solely through interaction with an axially symmetric chemical shift tensor and that the relaxation of C6 has contributions from both CSA and dipolar mechanisms. This figure demonstrates that for orientation of the C6-H internuclear vector close to 55° from the

Table I: Descriptions of Cholesterol Dynamics in EYPC Vesicles Consistent with ^{13}C NMR Data

						C5 line width (Hz)		C6 line width (Hz)		C6 T_1 (s)	
X_{CH}	r (Å)	τ_M[c] (μs)	$\tau_\parallel$ (ns)	$\tau_\perp$ (ns)	S	predicted[d]	exptl	predicted[e]	exptl	predicted[e]	exptl
0.2	114[a]	1.63	0.082	0.82	0.67	59	60 ± 5	60	60 ± 5	0.194	0.193 ± 0.018
	135[b]	2.71	0.085	0.85	0.52	59		60		0.194	
0.3	118[a]	1.81	0.14	1.4	0.71	72		75	75 ± 10	0.146	0.144 ± 0.016
	150[b]	3.71	0.15	1.5	0.50	74		76		0.144	
0.4	131[a]	2.48	0.25	2.5	0.77	119		122	120 ± 30	0.118	0.119 ± 0.047
	175[b]	5.89	0.25	2.5	0.50	118		121		0.117	

[a] Radii from Newman & Huang (1975). [b] Radii from Gent & Prestegard (1974). [c] η = 1.1 cP, T = 30 °C. [d] Relaxation through CSA mechanism; $\Delta\sigma$ = 170 ppm, $H_0 = 6.3T$. [e] Relaxation through CSA and dipolar mechanisms; $\Delta\sigma$ = 170 ppm, r = 1.09 Å, $H_0 = 6.3T$.

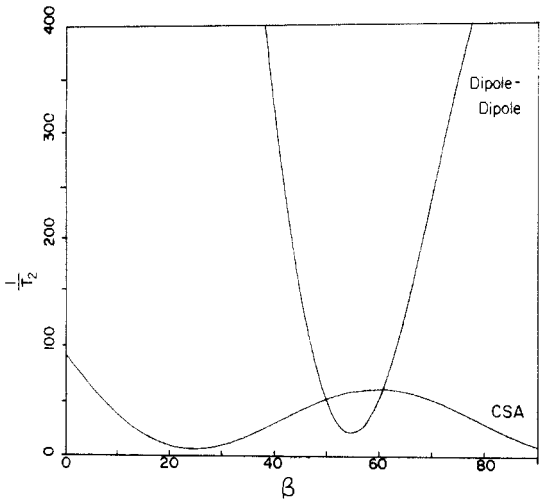

FIGURE 8: Comparison of spin–spin relaxation rates at 6.3T for CSA and dipolar mechanisms estimated for C6 of cholesterol as a function of β, the angle between the C6-H internuclear vector and the C_∞ axis of cholesterol (see text). $\tau_M = 10^{-6}$ s, $\tau_\parallel = \tau_\perp = 10^{-9}$ s, S = 0.7, $\Delta\sigma$ = 170 ppm, r = 1.09 Å.

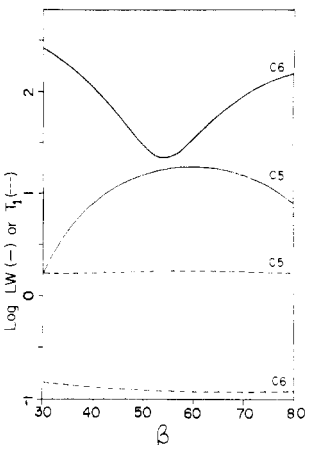

FIGURE 9: Semilog plots of line widths and spin–lattice relaxation times at 6.3T for C5 and C6 of cholesterol as a function of β, the angle between the C6-H internuclear vector and the C_∞ axis of cholesterol (see text). Parameters are as described in Figure 8.

C_∞ axis of cholesterol, C5 and C6 show quite similar natural line widths. It is of interest to note that although the calculated natural line widths for these two carbon resonances are similar, the spin–lattice relaxation time for C5 is significantly longer than that for C6. In ^{13}C NMR spectra at 6.3T of cholesterol in EYPC vesicles, the T_1 for C5 is considerably longer than that for C6 as evidenced by the greater attenuation of the C5 resonance by short pulse intervals (J. R. Brainard, unpublished experiments).

So far, our discussion has been limited to the *relative* magnitudes of line widths and spin–lattice relaxation times for cholesterol carbon resonances. While a unique quantitative description of the dynamics of cholesterol in sonicated vesicles is not possible at this time because of the uncertainties associated with estimating the direction and magnitudes of the chemical shift tensor and the paucity and quality of the experimental data, it is interesting to discuss what structural and dynamical information is consistent with the available ^{13}C NMR data. Table I contains parameters which describe the motion of cholesterol in sonicated EYPC–cholesterol vesicles of varying composition within the framework of our model. The lack of uniqueness of these parameters will be discussed below. This description was derived from the following considerations. We have assumed that the relaxation rates of cholesterol C5 and C6 may be estimated respectively by the effects of CSA and CSA plus dipole–dipole relaxation mechanisms using the geometry and chemical shift tensors described previously. The near equality of the line widths from C5 and C6 observed in 6.3T ^{13}C NMR spectra (Brainard & Cordes, 1981) suggests that the inclination of the C6-H internuclear vector is close to the magic angle; consequently, β was selected to be 55° in these calculations. Estimates for τ_M, the effective correlation times for vesicle rotation,[2] were derived from the Stokes–Einstein relationship and the reported Stokes radii for egg yolk phosphatidylcholine–cholesterol vesicles of varying composition (Newman & Huang, 1975; Gent & Prestegard, 1974) by using a solution viscosity of 1.1 cP and a temperature of 30 °C. The values of S, $\tau_\parallel$, and $\tau_\perp$ were obtained from the ^{13}C relaxation data by first varying S to predict the experimental line width for C6 and then setting $\tau_\perp/\tau_\parallel = 10$ and varying $\tau_\parallel$ to predict the spin–lattice relaxation time. The order parameters obtained in this way must be regarded as upper bounds since the experimental line widths include instrumental and data-processing contributions. Several observations concerning Table I are noteworthy. First, in order to model the decrease in spin–lattice relaxation times, it is necessary to decrease the rates of motions of the cholesterol molecule within the vesicle as the cholesterol content increases. Second, using the Stokes radii derived from the data of Newman and Huang, it is necessary to increase the order parameter for the long axis of the cholesterol molecule in order to predict the change in line width with increasing concentrations of cholesterol.

It is also interesting to compare the order parameters for cholesterol in sonicated vesicles with those reported by Oldfield et al. (1978) for cholesterol-3-d_1 in unsonicated DMPC lipo-

[2] We have chosen to neglect the contribution to τ_M from the translational diffusion of cholesterol since its magnitude, estimated from lipid translational diffusion constants (Edidin, 1974), is only 10% of that from vesicle rotation. In addition, Newman & Huang (1975) reported no Stokes radii for vesicles containing more than 30% cholesterol, since their data indicated that those vesicles were not spherical. Nevertheless, we have estimated the Stokes radius for X_{CH} = 0.4 from their reported diffusion coefficient, assuming a spherical shape.

somes. Direct comparison of these results might seem inappropriate since the deuterium and carbon experiments were performed on bilayers composed of different phosphatidylcholines. However, both measurements were made at approximately 40 °C above the respective gel to liquid-crystalline phase transition temperature. The order parameters in Table I calculated with radii derived from the data of Newman and Huang are quite similar to those reported by Oldfield et al. (1978). For example, at $X_{CH} = 0.3$, the order parameters are 0.71 and 0.66 for C6 cholesterol and cholesterol-3-d_1, respectively. We emphasize, however, that the values derived for S from the line widths are extremely sensitive to the magnitude of τ_M. If we use the values reported by Gent and Prestegard for the Stokes radii of egg yolk phosphatidylcholine vesicles containing increasing amounts of cholesterol, the observed line-width increases are predicted by the increases in vesicle rotational correlation time alone, and the derived order parameters are almost invariant with cholesterol content, suggesting that the lipid order in sonicated vesicles is essentially independent of X_{CH}. In addition, the magnitudes of the order parameters are reduced to approximately 0.5, which are significantly smaller than those of Oldfield et al. (1978). Consequently, the resolution of questions concerning the relative contributions to relaxation rates from the effects of increasing vesicle size and from the effects of cholesterol upon the order parameter and those questions concerning possible differences in the structural organization of unsonicated and sonicated lipid bilayers await more extensive and precise experimental data.

The ratio $\tau_\perp/\tau_\parallel = 10$ is not unique. The data are fit equally well with ratios from 1 to 1000. For example, $\tau_\parallel = 0.07$ ns, $\tau_\perp = 7.0$ ns, $S = 0.67$, and $\tau_\parallel = \tau_\perp = 0.16$ ns, $S = 0.67$ reproduce the experimental data for $X_{CH} = 0.2$, $r_0 = 114$ Å as well as the parameters given in Table I. We note that, although $\tau_\perp$ may vary widely, $\tau_\parallel$ is reasonably well defined. In general, the values for $\tau_\parallel$ derived from these ^{13}C NMR measurements are 3–4 times smaller than reported correlation times for rotation of the spin-labeled sterol analogue 3-doxylcholestane in phospholipid bilayers (Schreier et al., 1978). In light of the approximations made in obtaining these correlation times, the agreement is satisfactory.

It should be emphasized that when $\tau_\parallel \leq \tau_\perp < \tau_M$ (i.e., the motions of cholesterol within the bilayer are at least an order of magnitude faster than vesicle rotation) the derived order parameter is independent of the ratio $\tau_\perp/\tau_\parallel$. However, when $\tau_\perp$ approaches τ_M, the data are fit only if S is decreased. For example, $\tau_\parallel = 0.07$ ns, $\tau_\perp = 700$ ns, and $S = 0.45$ fit $X_{CH} = 0.2$ when $r_0 = 114$ Å. In the extreme case where $S = 0$ (i.e., the cholesterol C_∞ axis is spatially unrestricted), the data for $X_{CH} = 0.2$ are fit when $\tau_\parallel = 0.07$ ns and $\tau_\perp = 1.4$ μs. Note that $\tau_\perp \simeq \tau_M$ and $\tau_\perp/\tau_\parallel = 20\,000$. This seems physically unreasonable for cholesterol in a lipid bilayer.

For completeness, however, we mention that a 30-fold or greater difference in the rate of motion of and about the C_∞ axis of a probe (i.e., $\tau_\perp/\tau_\parallel > 30$) will also result in significantly narrower line widths for methine carbons whose ^{13}C-H vector is inclined close to 55° from the C_∞ axis as compared to line widths of other methine carbons. This is true even if the motion of the C_∞ axis is spatially unrestricted (i.e., $S = 0$). Consequently, the geometry of the interaction vector may still be of great importance in systems (e.g., nucleic acids) where there is little or no "order", if there is anisotropic motion characterized by unequal rates about different rotational axes. For cholesterol in sonicated vesicles, the motion of the C_∞ axis is likely to be significantly hindered (i.e., $S \neq 0$) due to the liquid-crystalline nature of the lipid bilayer. We believe that this spatial restriction is the major source of the anisotropy in the motion of cholesterol, which together with fast rotation about the C_∞ axis and the orientation of the pertinent interaction vectors results in the magic angle effect.

The purpose of this paper has been to relate the geometry and dynamics of an axially symmetric probe in a membrane to nuclear magnetic relaxation rates. We have treated the case where the relevant interaction vector is not coaxial with the major symmetry axis of the probe so that both motions of and motions about this axis contributed to nuclear magnetic relaxation. Although the formulism developed here has been applied to cholesterol in phospholipid membranes, it may easily be adapted to provide information about the dynamics and geometry of nuclear magnetic probes where the motions responsible for relaxation can be adequately described by the physical models presented in Figures 1 and 2.

After this paper had been submitted for publication, Richarz et al. (1980) published a treatment of the situation shown in Figure 2 within the framework of the diffusion in the cone model. Their approximate expression for the correlation function differs from our eq 15 when this equation is specialized to the diffusion in the cone model (i.e., $S \rightarrow S_{cone}$). Their expression has the unsatisfactory feature that in the limit that $\theta_0 \rightarrow 0$ ($S_{cone} \rightarrow 1$), the wobbling diffusion constant, D_w, does *not* drop out, and, hence, their result does not rigorously reduce to eq 18 [i.e., their expression, in contrast to ours, does not have property (1)]. In spite of this difference, the two expressions can lead to similar numerical results in a number of cases of interest. In this paper, we have stressed that it is difficult to relate effective correlation times to diffusion constants. We believe that the way this is done by Richarz et al. is not satisfactory.

Acknowledgments

J.R.B. gratefully acknowledges the helpful comments, encouragement, and support of Drs. Eugene Cordes and Joel Morrisett. We have benefited from conversations with Dr. Dennis Torchia.

References

Appleman, B. R., & Dailey, B. P. (1974) *Adv. Magn. Reson. 7*, 231–320.

Avila, E. M., Hamilton, J. A., Harmony, J. A. K., Allerhand, A., & Cordes, E. H. (1978) *J. Biol. Chem. 253*, 3983–3987.

Bocian, D. F., & Chan, S. I. (1978) *Annu. Rev. Phys. Chem. 29*, 307–335.

Brainard, J. R., & Cordes, E. H. (1981) *Biochemistry* (preceding paper in this issue).

Brink, P. M., & Satchler, G. R. (1961) *Angular Momentum*, 2nd ed., Oxford University Press, London.

Brown, M. F., Seelig, J., & Häberlen, U. (1979) *J. Chem. Phys. 70*, 5045–5053.

Edidin, M. (1974) *Annu. Rev. Biophys. Bioeng. 3*, 179–201.

Gally, H. U., Seelig, A., & Seelig, J. (1976) *Hoppe-Seyler's Z. Physiol. Chem. 357*, 1447–1450.

Gent, M. P. N., & Prestegard, J. H. (1974) *Biochemistry 13*, 4027–4033.

Gent, M. P. N., & Prestegard, J. H. (1977) *J. Magn. Reson. 25*, 243–262.

Hamilton, J. A., & Cordes, E. H. (1978) *J. Biol. Chem. 253*, 5193–5198.

Hamilton, J. A., Oppenheimer, H., & Cordes, E. H. (1977) *J. Biol. Chem. 252*, 8071–8080.

Hamilton, J. A., Cordes, E. H., & Glueck, C. J. (1979) *J. Biol. Chem. 254*, 5435–5441.

Howarth, O. W. (1979) *J. Chem. Soc., Faraday Trans. 2 75*, 863-873.
Kinosita, K., Kawato, S., & Ikegami, A. (1977) *Biophys. J. 20*, 289-305.
Lipari, G., & Szabo, A. (1980) *Biophys. J. 30*, 489-506.
Lipari, G., & Szabo, A. (1981) *J. Chem. Phys.* (in press).
Newman, G. C., & Huang, C. (1975) *Biochemistry 14*, 3363-3369.
Norton, R. S., Clouse, A. O., Addleman, R., & Allerhand, A. (1977) *J. Am. Chem. Soc. 99*, 79-83.
Oldfield, E., Meadows, M., Rice, R., & Jacobs, R. (1978) *Biochemistry 17*, 2727-2740.
Petersen, N. O., & Chan, S. I. (1977) *Biochemistry 16*, 2657-2667.
Richarz, R., Nagayama, K., & Wüthrich, K. (1980) *Biochemistry 19*, 5189.
Schreier, S., Polnaszek, C. F., & Smith, I. C. P. (1978) *Biochim. Biophys. Acta 515*, 375-436.
Seelig, J. (1977) *Q. Rev. Biophys. 10*, 353-418.
Seiter, C. H. A., & Chan, S. I. (1973) *J. Am. Chem. Soc. 95*, 7541-7553.
Stockton, G. W., Polnaszek, C. F., Tulloch, A. P., Hasan, F., & Smith, I. C. P. (1976) *Biochemistry 15*, 954-966.
Wallach, D. (1967) *J. Chem. Phys. 47*, 5258-5268.
Wittebort, R. J., & Szabo, A. (1978) *J. Chem. Phys. 69*, 1722-1736.
Woessner, D. E. (1962a) *J. Chem. Phys. 36*, 1-4.
Woessner, D. E. (1962b) *J. Chem. Phys. 37*, 647-654.

Mössbauer Spectroscopic Studies of Hemerythrin from *Phascolosoma lurco* (syn. *Phascolosoma arcuatum*)†

Paul E. Clark and John Webb*

ABSTRACT: Hemerythrin from coelomic cells of *Phascolosoma lurco* (syn. *P. arcuatum*) was isolated by gel filtration as two components, hemerythrin-I (25%) and hemerythrin-II (75%). The Mössbauer spectrum of oxyhemerythrin-II consisted of two pairs of lines of the same isomer shift (0.5 mm s^{-1}) corresponding to Fe(III) but different quadrupole splitting (1.01 and 2.02 mm s^{-1}). Application of a 2.5-T magnetic field at 4.2 K caused no significant spectral broadening. The $2Fe{\cdot}O_2$ binding site thus contains two nonequivalent high-spin Fe(III) ions that are antiferromagnetically coupled. The Mössbauer spectra of the minor component, hemerythrin-I, indicated an identical binding site. On deoxygenation, the spectrum was dominated by a simple quadrupole split doublet corresponding to Fe(II), indicating that the binding site in this derivative contains two identical Fe(II) ions that interact only weakly, if at all. The Mössbauer spectra of azidohemerythrin-II indicated that this derivative also contains a pair of antiferromagnetically coupled Fe(III) ions with the same isomer shift (0.5 mm s^{-1}) but quadrupole splittings (1.40 and 1.96 mm s^{-1}) that are not identical with those in oxyhemerythrin.

Hemerythrin, the oxygen-transport protein found in several phyla of marine invertebrates, binds dioxygen in the stoichiometry of $2Fe:O_2$. Many investigations using a wide range of biochemical, spectroscopic, and magnetic studies have been designed to elucidate the nature of the dioxygen binding site. Notwithstanding this extensive series of reports, the structure of the dioxygen binding site is still uncertain and controversial, as recounted in recent reviews (Okamura & Klotz, 1973; Klotz et al., 1976; Kurtz et al., 1977; Stenkamp & Jensen, 1979; Loehr & Loehr, 1979; Klippenstein, 1980).

Detailed structures for the binding site have been proposed on the basis of X-ray studies of metazidohemerythrin from *Themiste* (syn. *Dendrostomum*) *zostericola*, formerly known as *T. pyroides* (Hendrickson et al., 1975; Hendrickson & Ward, 1977), metazidohemerythrin from *Phascolopsis* (syn. *Golfingia*) *gouldii* (Ward et al., 1975), and metaquohemerythrin from *T. dyscritum* (Stenkamp et al., 1976a,b, 1978a,b). The differences among these structures have been reviewed in detail recently (Stenkamp & Jensen, 1979). In summary, two structures have been proposed: first, the metaquohemerythrin structure, which involves a (face-sharing) pair of octahedrally coordinated Fe(III) centers that share a face via oxygens from a water molecule and an asparate and glutamate side chain, and second, the metazidomohemerythrin structure, which also contains two octahedrally coordinated Fe(III) centers but now joined by a single μ-oxo bridge. Recent refinements of the crystallographic data have reduced the differences between the two models, with the confacial bioctahedron now containing a Fe–O–Fe bridging unit (J. Sanders-Loehr, personal communication).

In this paper we report results of Mössbauer studies of hemerythrin isolated from coelomic cells of a different species from those mentioned above, namely, *Phascolosoma lurco* (syn. *P. arcuatum*) (Stephen & Edmonds, 1972).

Mössbauer spectroscopy has been used extensively in studies of the hemerythrin dioxygen binding site for it is a particularly appropriate technique for detecting the presence of magnetic interaction between iron atoms (Trautwein, 1974; Johnson, 1975; Webb, 1975). Antiferromagnetic coupling between iron atoms in derivatives of several hemerythrins has been demonstrated clearly in previous studies (Okamura et al., 1969; York & Bearden, 1970; Trautwein, 1974; Garbett et al., 1974). The present study compares the electronic environment of the two iron atoms in two components of oxyhemerythrin isolated from *P. lurco* as well as the deoxy and azido derivatives of the major component.

Experimental Procedures

Preparation of Hemerythrin. Oxyhemerythrin was isolated from the coelomic cells of approximately 200 specimens of *P. lurco* collected less than 24 h previously from the mangrove swamps of the Brisbane River, Queensland, Australia. The

† From the Department of Physics, Monash University, Clayton, Victoria, Australia 3168 (P.E.C.), and the School of Mathematical and Physical Sciences, Murdoch University, Murdoch, Western Australia, Australia 6150 (J.W.). *Received November 14, 1980.* Financial support from the Australian Research Grants Committee and Murdoch University Special Research Grants is gratefully acknowleged.

0006-2960/81/0420-4628$01.25/0